Physica A 194 (1993) 415–423
North-Holland

PHYSICA A

Freezing of binary mixtures of hard-sphere colloids

P. Bartlett[a,1] and P.N. Pusey[b]

[a]*School of Chemistry, University of Bristol, Bristol BS8 1TS, UK*
[b]*Department of Physics, University of Edinburgh, Mayfield Road, Edinburgh EH9 3JZ, UK*

Binary mixtures of suspended colloidal spheres of size ratio $\alpha = 0.58$, whose interaction is close to that of hard spheres, undergo freezing transitions into ordered superlattice structures. At different number ratios of the two species, both the AB_2 (atomic analogue AlB_2) and the AB_{13} (atomic analogue $NaZn_{13}$) structures are found. The structures were identified by both "powder light crystallography" and electron microscopy of dried samples. The phase diagram contains three eutectics. The freezing transitions in this conceptually simple binary mixture are driven entropically: put simply, at a given concentration and number ratio, the system adopts the "most efficient" packing of the spheres.

1. Introduction

The idea that the structure of "simple" condensed phases is determined predominantly by packing constraints is very old and derives essentially from the work of van der Waals [1]. The dominant role of the short-ranged repulsive forces was most directly demonstrated by the discovery, from computer simulation studies [2], that a purely repulsive hard sphere system has a first order fluid–solid phase transition. While the one-component system of hard spheres studied by Alder and Wainwright froze into a close-packed face-centred-cubic structure, recent work has shown, rather surprisingly, that there exists a wide variety of other ordered (and partially ordered) phases which can be stabilized similarly by pure excluded volume factors. For example, simulation studies [3] suggest that, at high densities, a system of anisotropic hard core particles may form spontaneously a number of common liquid crystalline phases (including nematics, smectics and columnar structures). Here we explore an alternative route to structural complexity. The aim of the present paper is to demonstrate that complex superlattice structures are stable at high densities in binary mixtures of differently sized hard spheres. In this expanded

[1] Author to whom correspondence should be addressed. Fax: (272) 251295; Telephone: (272) 303030, ext. 4267; E-mail (Janet): Bartlettp@UK.AC.BRISTOL.SIVA.

version of an earlier paper [4] we show that a dense mixture of hard sphere colloids of size ratio $\alpha = \sigma_B/\sigma_A = 0.58$ (where σ_A and σ_B are the diameters of the large (A) and small (B) spheres) may form either one of two different superlattice structures, AB_2 and AB_{13}, depending upon the initial conditions.

The colloidal particles used in this work consisted of spherical poly(methyl methacrylate) (PMMA) cores stabilized against aggregation by a thin (~10 nm), chemically grafted, layer of poly(12-hydroxy stearic acid) [5]. Particle diameters were $\sigma_A = 642 \pm 5$ nm and $\sigma_B = 372 \pm 5$ nm. Experiment shows that these composite particles readily disperse in hydrocarbons as essentially uncharged spheres. In the current work the particles were suspended in mixtures of cis-decalin and carbon disulphide in proportions chosen so that the refractive index of the mixture approximately matched that of the particles (~1.51). In this way the van der Waals attractive forces were minimized and the interparticle potential is essentially zero until the separation is reduced to the point at which the grafted polymeric layers first touch. Any closer approach of the two colloidal particles requires the polymeric layers to either compress or interpenetrate. Both theory (for a review of the properties of polymeric brushes, see ref. [6]) and experiment [7] demonstrate that the free energy penalty for any significant distortion of the polymeric layer is large compared with kT. Consequently the colloid interparticle potential is steeply repulsive and may be approximated well by that of a hard sphere. This has been confirmed by measurements made on the phase behaviour [8,9], crystallization [10] and glass formation [11] in one-component suspensions of this type.

2. Superlattice phases

Our most striking finding is that in mixtures of $\alpha = 0.58$ *two* different superlattice phases appear to be stable. Each phase is observed at different ratios, N_B/N_A of the numbers of the two colloidal species. We consider first the AB_2 structure which was observed in suspensions with number ratios N_B/N_A of 4 and 6 and total volume fractions $\phi_A + \phi_B$ between 0.525 and 0.557. Crystallization was noticeably slower in these binary mixtures compared to the one-component systems previously studied [8,9] with crystals being clearly visible only after about five weeks after mixing (cf. a few hours for the one-component system in ref. [8]). Fig. 1a shows an electron micrograph image of the crystalline phase formed in a sample with the composition $N_B/N_A = 6$ and the original total density $\phi_A + \phi_B = 0.536$. The most notable feature is the binary long range order with an alternating sequence of planes of large and small spheres being clearly visible. This micrograph is consistent with an (011)

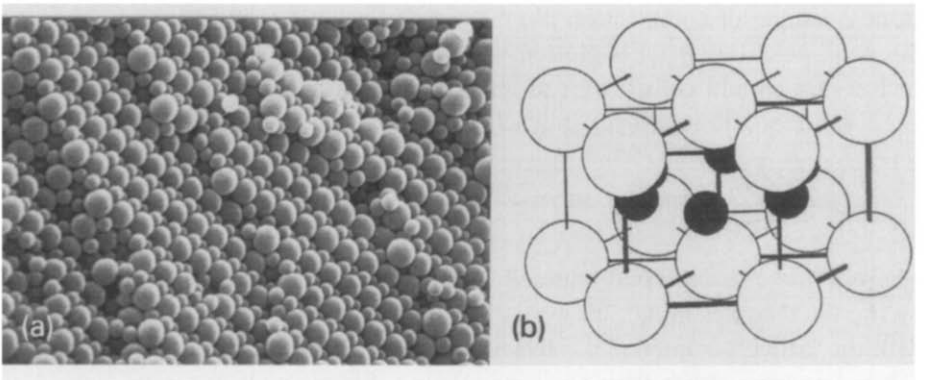

Fig. 1. (a) Scanning electron microscopy image of the AB_2 superlattice, found in a sample with the original composition $N_B/N_A = 6$ and $\phi_A + \phi_B = 0.536$. The micrograph shows an approximate (011) section. (b) Structure of the AB_2 phase. The hexagonal unit cell is shown in bold.

section through the AB_2 structure depicted in fig. 1b. This is a layered structure, akin to AlB_2, with the large and small spheres residing in alternating close-packed planes. In the hexagonal unit cell the larger A spheres are stacked vertically above one another along the c-axis, while the smaller B spheres occupy the trigonal prismatic cavities between neighbouring A layers.

Further evidence for the formation of the AB_2 structure comes from light diffraction measurements. Fig. 2a shows the indexing of the diffraction data

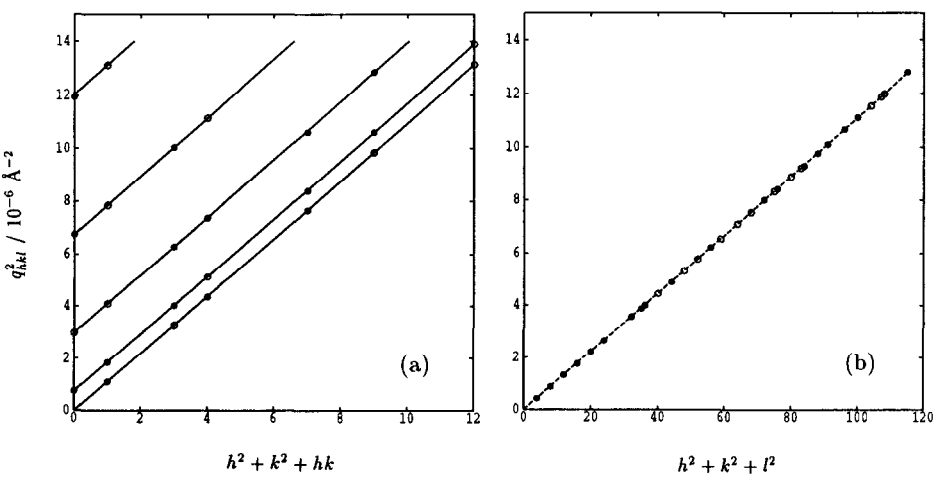

Fig. 2. Powder diffraction data. (a) Indexing the AB_2 phase. The square of the peak position q^2_{hkl} is plotted as a function of $h^2 + k^2 + hk$. The solid lines represent the theoretical result for a hexagonal phase of dimensions $a = 693$ nm and $c = 724$ nm, with the index l increasing from $l = 0$ (bottom right) to 4 (top left). The filled points denote the positions of observed Bragg reflections while unobserved reflections are indicated by the unfilled circles. (b) Indexing the AB_{13} phase. The dashed line corresponds to the cubic lattice constant $a = 1884$ nm.

from a sample of composition $N_B/N_A = 4$ and $\phi_A + \phi_B = 0.533$. The square of the peak position (q^2_{hkl}) is plotted versus $h^2 + k^2 + hk$. For a hexagonal phase such a plot should consist of a series of straight lines, each corresponding to a fixed value of the interlayer index l,

$$q^2_{hkl} = \frac{16\pi^2}{3a^2}(h^2 + k^2 + hk) + \frac{4\pi^2}{c^2} l^2 , \tag{1}$$

where a and c are the two unit cell lengths. A total of 15 Bragg peaks (shown by the filled circles in fig. 2a) were observed which index on a hexagonal phase with the lattice parameters $a = 693$ nm and $c = 724$ nm ($c/a = 1.045$). Although a few lines are either very weak or missing, for example the reflections 110, 201, 002 and 102, there seems to be no systematic absences, as indeed expected for the AB_2 structure (space group P6/mmm (Q^{191})). Unfortunately we are not able to quantitatively analyse the intensity data because of our present lack of detailed knowledge on the form factors of the individual particle species near refractive-index match. So consequently while the AB_2 structure is the most plausible hexagonal phase, the precise details of the local structure must await further experiments. Finally, we note that assuming the unit cell contains just one large and two small spheres gives the crystal density as $\phi_A + \phi_A = 0.638$.

Suspensions prepared with compositions $N_B/N_A = 9$, 14, 20 and 30 crystallized into a second superstructure with the stoichiometry AB_{13}. Crystallization was rapid compared to AB_2 with crystallites of AB_{13} being visible within a few days of sample preparations. Fig. 3a shows a drawing of the proposed structure of this cubic phase. The structure is essentially similar to

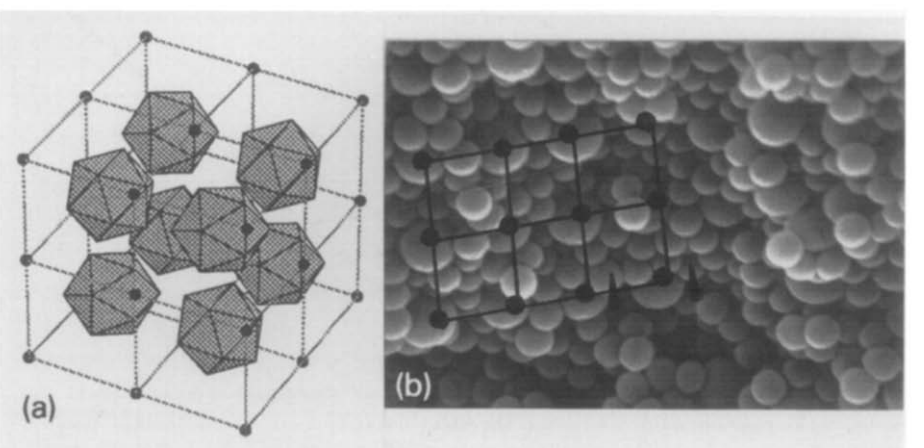

Fig. 3. (a) Proposed structure of the AB_{13} phase. (b) Electron micrograph of AB_{13} from a sample of original composition $N_B/N_A = 14$ and density $\phi_A + \phi_B = 0.553$.

that commonly found for binary metal alloys of composition AB_{13}, such as $NaZn_{13}$ and UBe_{13}. The unit cell consists of eight icosahedra clusters of small spheres, each of which has at its centre an additional small sphere, arranged within a cubic lattice of large spheres. As is apparent from fig. 3a the icosahedra are orientationally ordered with each neighbouring polygon of small spheres rotated by $\pi/2$ about the crystallographic x-axis. The corresponding space group is $Fm\bar{3}c$ (Q^{226}).

Strong evidence for the formation of this remarkably complex structure comes from light scattering measurements. The diffraction data from the crystalline phase formed in a mixture with composition $N_B/N_A = 14$ and density $\phi_A + \phi_B = 0.539$ is shown in fig. 2b, as a plot of q_{hkl}^2 versus $h^2 + k^2 + l^2$. For a cubic phase, such a plot should pass through the origin and be linear with the slope $4\pi^2/a^2$ where a is the unit cell dimension. A total of 19 distinct Bragg reflections were observed which index on a face centred cubic phase of lattice constant $a = 1884$ nm with the extinction symbol [12] F--c. There were no unobserved reflections below $hkl = 620$. There are only two space groups consistent with this data, namely $F\bar{4}3c$ (Q^{219}) and $Fm\bar{3}c$ (Q^{226}) which differ in the presence ($Fm\bar{3}c$) or absence ($F\bar{4}3c$) of an inversion centre. To distinguish between these two possibilities requires measurements of the absolute intensity of the reflections $I(hkl)$, particularly those with hkl all odd. Unfortunately, because of the problems discussed above, we are currently not able to do this and so on the basis of the powder diffraction data alone we cannot differentiate between the space groups $F\bar{4}3c$ (Q^{219}) and $Fm\bar{3}c$ (Q^{226}).

Support for the more symmetric AB_{13} structure Fm3c (Q^{226}) comes from electron microscopy. Fig. 3b shows an example of the structures found. Clearly the drying of the sample has disrupted much of the original order. However a reasonably well ordered array of 12 large spheres (shown by the grid in fig. 3b), comprising part of the (011) face of the AB_{13} unit cell, is still visible. Indeed a close inspection of fig. 3b reveals two pentagons of small spheres (arrowed in fig. 3b) resulting from the cleavage of the icosahedron of small spheres.

3. Phase diagram

The positions of these superlattice phases within the binary phase diagram were determined by observations made on some 25 samples prepared at seven fixed values of composition $N_B/N_A = 2$, 4, 6, 9, 14, 20 and 30. The surprising finding was that superlattice structures formed over a wide range of suspension compositions. Indeed a stable phase of either AB_2 or AB_{13} was found at all compositions studied except for suspensions with $N_B/N_A = 2$, which showed,

rather unexpectedly, no observable crystallization during the course of our experiments.

The densities of the superlattice phases formed at the fluid–solid phase boundary show a systematic variation as a function of the initial suspension number ratio N_B/N_A, which is illustrated in fig. 4a. Clearly, as one can best see

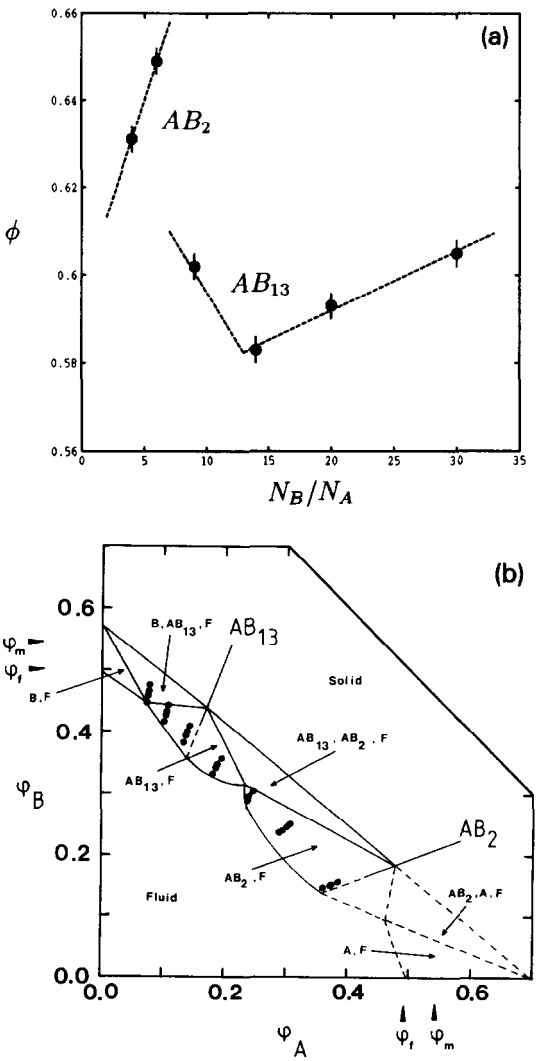

Fig. 4. (a) Densities of the superlattice phases as a function of the composition, N_B/N_A, of the suspension from which they crystallized. The data is for samples located within the two-phase region of fluid–solid coexistence. (b) Constant volume phase diagram. The points represent the samples studied. The approximate phase boundaries are marked by the solid lines; the region around $N_B/N_A = 2$ is shown dashed because no crystallization was observed in our experiments.

from the AB_{13} data, the compound phases are most stable (and thus form at the lowest densities) at the stoichiometric composition. Any deviations from this ideal stoichiometry tends to destabilize the resulting crystal which shifts the solid phase boundary to higher densities. This fact, combined with the different symmetries of the two superlattice structures, suggests that the equilibrium phase diagram will most probably be eutectic in form.

Since colloidal systems are generally studied at essentially constant volume the binary phase diagram is most naturally discussed in terms of the partial volume fractions, ϕ_A and ϕ_B, of the two components. This constant volume representation has several convenient properties: first, samples with a constant number fraction lie on lines radiating from the origin whereas samples with a fixed total volume fraction, $\phi_A + \phi_B$, form straight lines which intersect the ϕ_A and ϕ_B axes at $\pi/4$; second, the volumes of the coexisting phases can be readily calculated from simple geometric arguments [13]. Fig. 4b shows a plausible form for the phase diagram which encompasses our current results. A striking feature is its complexity. The diagram contains four stable solid phases; the two superlattice structures (AB_2 and AB_{13}) which we have observed in this work, and crystals of both A and B which must be stable structures at the extreme limits of composition. In between each of these limiting compositions there is a constant-volume eutectic [13]. With an assumption of complete solid immiscibility the phase diagram contains four regions of two-phase fluid–solid equilibrium (labelled by the coexisting phases in fig. 4b) and three triangular three-phase regions (describing, for instance, the equilibria between AB_2, A, and a fluid phase). As can be seen from fig. 4b the current samples lie in the two-phase AB_2, fluid and AB_{13}, fluid regions and the three-phase eutectic between AB_{13}, B, and fluid. Consequently the exact structure of the phase diagram outside these regions must await further experiments.

4. Comparison with theory

In recent years the nature of the hard-sphere phase transition has been considerably clarified by the application of density functional arguments [14]. From these theories it is clear that the stability of the hard-sphere crystal is a result of a rather delicate balance between configurational and correlational entropy. While at low densities configurational entropy favours the disordered fluid state, with an increase in density correlational terms become increasingly dominant and ultimately stabilize the crystal at the highest densities. Physically, localization results in a *gain* in correlation entropy since the additional "free-volume" in the crystal allows each particle to reduce its interactions with its neighbours by moving further apart. In a binary system, by the same token,

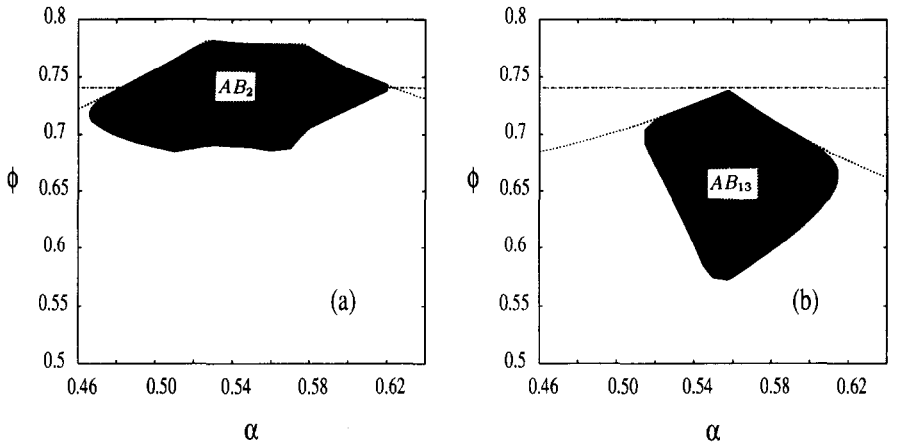

Fig. 5. Free-volume predictions for the regions where (a) AB_2 and (b) AB_{13} phases are stable with respect to a solid state phase separation into crystals of pure A and B. The dotted lines indicate the maximum close-packed densities (ϕ_m). The dot–dashed lines denote the close-packed density of the one-component fcc crystal ($\phi_{cp} = 0.7405$) and are shown for reference.

one would expect the stable crystal phases to be those in which the constituent spheres are packed so as to maximize the "free-volume".

The packing efficiency of a number of ordered binary structures has been explored by Murray and Sanders [15]. For the size ratios relevant here they found only two structures, AB_2 and AB_{13}, which have maximum densities comparable to the close-packed packing fraction of the pure component phases ($\phi_{cp} = 0.7405$). For $\alpha = 0.58$ the maximum packing fractions of these two structures are $\phi_m(AB_2) = 0.776$ and $\phi_m(AB_{13}) = 0.713$. Accordingly Murray and Sanders concluded from purely geometric arguments that while the AB_2 structure should be stable, the AB_{13} phase will be unstable with respect to a phase separation into pure A and B phases.

The stability of the ordered AB_2 and AB_{13} phases are currently being investigated by computer simulation [16]. In the absence of these detailed calculations we describe the results of a simple free-volume model [17] which appears to agree reasonably well with the experimental data described above and in ref. [4]. Fig. 5 shows the predictions for the regions where the AB_2 and the AB_{13} phases are stable with respect to a solid separated mixture of pure A and B crystals. We see that while both phases are predicted to be stable at a size ratio of $\alpha = 0.58$ the AB_{13} phase is stable at appreciably lower overall densities (as is indeed seen in the data of fig. 4a).

References

[1] J.D. van der Waals, On the Continuity of the Gaseous and Liquid States, J.S. Rowlinson, ed., Studies in Statistical Mechanics, vol. XIV (North-Holland, Amsterdam, 1988).
[2] B.J. Alder and T.E. Wainwright, J. Chem. Phys. 27 (1957) 1208.
[3] D. Frenkel, in: Liquids, Freezing and the Glass Transition, Les Houches, Session LI, D. Levesque, J-P. Hansen and J. Zinn-Justin, eds. (Elsevier, Amsterdam, 1991) p. 689.
[4] P. Bartlett, R.H. Ottewill and P.N. Pusey, Phys. Rev. Lett. 68 (1992) 3801.
[5] L. Antl, J.W. Goodwin, R.D. Hill, R.H. Ottewill, S.M. Owens, S. Papworth and J.A. Waters, Colloid. Surf. 17 (1986) 67.
[6] S.T. Milner, Science 251 (1991) 905.
[7] R.J. Cairns, R.H. Ottewill, D.W. Osmond and I. Wagstaff, J. Colloid Interface Sci. 54 (1976) 45.
[8] P.N. Pusey and W. van Megen, Nature 320 (1986) 340.
[9] S.E. Paulin and B.J. Ackerson, Phys. Rev. Lett. 64 (1990) 2663.
[10] P.N. Pusey, W. van Megen, P. Bartlett, B.J. Ackerson, J.G. Rarity and S.M. Underwood, Phys. Rev. Lett. 63 (1989) 2753.
[11] W. van Megen and P.N. Pusey, Phys. Rev. A 43 (1991) 5429; W. van Megen, S.M. Underwood and P.N. Pusey, Phys. Rev. Lett. 67 (1991) 1586.
[12] T. Hahn, ed., International Tables for Crystallography, vol. A (Reidel, Dordrecht, 1983).
[13] P. Bartlett, J. Phys.: Condens. Matter 2 (1990) 4979.
[14] M. Baus and J.L. Colot, Mol. Phys. 55 (1985) 653; W.A. Curtin and N.W. Ashcroft, Phys. Rev. A 32 (1985) 2909.
[15] M.J. Murray and J.V. Sanders, Philos. Mag. A 42 (1980) 721.
[16] M.D. Eldridge and P.A. Madden, preprint (1992).
[17] P. Bartlett, to be published.